BAW-10247Q4NP
Revision 0

**Response to Request for
Additional Information – BAW-10247(P)**

August 2007

AREVA

AREVA NP Inc.

BAW-10247Q4NP
Revision 0

Response to Request for

Additional Information – BAW-10247(P)

Table of Contents

This document contains a total of 94 pages.

Second Round of RAIs on RODEX4 Documents
(BAW-10247, EMF-2994, and EMF-3014)

To assist in the review process, two sets of tables have been provided below independent of any specific RAI question. The first set of tables provide a summary of the changes that have been made to the RODEX4 code and proposed changes to the methodology since the original submittal of BAW-10247(P) back in August of 2004. The second set of tables provides a complete listing of all the various parameters that are considered in the statistical methodology and the uncertainties that are applied to them.

RODEX4 Methodology Changes

The following table lists the changes to the RODEX4 statistical methodology that have been proposed since the original submittal of BAW-10247(P) in August of 2004.

Table A – RODEX4 Methodology Changes since Original Submittal

RODEX4 Code Changes

Since the original submittal of BAW-10247 for review in August of 2004, the RODEX4 code has been changed to address issues identified during the review process. Four new code versions have been made, versions UAPR05, UOCT06, UNOV06, and UJUN07, each of which contained multiple changes. Some of these changes were implemented to fix errors and others were made to add calculational flexibility needed to respond to RAIs. The following table lists the pertinent changes and provides a brief discussion of their impact.

Table B – RODEX4 Code Modifications since Original Submittal

Table C – Steady State Uncertainty Summary

Slow Transient Uncertainty Parameters

Table D – Slow Transient Uncertainty Summary

Fast Transient Uncertainty Parameters

Table E – Fast Transient Uncertainty Summary

Summary Comparison of the Realistic and Old Methodologies

The margin gains and losses to the transition to the new methodology should be generally applicable. The steady state results provided below were taken from the BWR-6 sample case and from the BWR-4 EPU cases for the steady state and transient results. In some cases, improved LHGR limits may be achieved.

Table F – Summary Comparison of Realistic and Old Methodology (from response 3)

General Comment:

In general, there has been little justification for the uncertainty values that have been selected. In particular, for model parameters, there should be plots showing that the model at its upper and lower limits, bound a large portion (95/95) of the data. Please keep this in mind when responding to the following RAIs and, whenever possible, demonstrate <u>quantitatively</u> that the selected uncertainty values sufficiently bound the measured data.

Question 1:

The responses provided in the November, 2006 letter did not provide the results from the sensitivity analyses requested in RAI# 23 from the first round of RAIs. The first round RAI #23 requested that sensitivity analyses be provided on those RODEX4 model uncertainties not considered in the methodology but this request did not provide many specifics. The current request is intended to supplement the first round RAI# 23 and provide specifics on the sensitivity analyses that should be provided. Please perform the following sensitivity analyses for rod pressure and strain increments as a function of burnup for the BWR-4 equilibrium core and document the results in a table similar to Table 1.1;

a) Assume the mean fuel thermal expansion is biased 4% higher than RODEX4 assumed[b]
b) Assume there is a 30% (95/95) uncertainty in solid swelling and how these impact rod pressure, cladding strain and strain increment calculations.
c) Please determine the uncertainty in rod growth based on the limited axial irradiation growth data and perform a sensitivity analysis to determine the effect of irradiation growth on rod pressure calculations.
d) The slow transient analyses also have no [   ] model even though it may impact the slow transient strain analysis. In addition, there is considerable uncertainty in this model due to the small amount of data used to verify this model and the large variability in the data used to develop this model.
    Please perform slow transient analyses assuming the uncertainty in this model is 40% (95/95).
e) The slow transient analysis also does not consider the [

                            ] . Please perform this analysis using the same uncertainties for these parameters as used for the fast transient conditions.

Perform each of the listed analyses individually and provide the information indicated in Table 1.1. For all the sensitivity analyses that require a strain value, please list both the total strain (elastic + permanent) and the permanent strain.

Based on the requested sensitivity analyses, please provide a justification of why the uncertainties in these model parameters are not included (Section 2.3.4).

---

[b]   The FRAPCON-3 thermal expansion differs from the RODEX4 expansion by 4% within given temperature ranges. In addition, the standard deviation on the thermal expansion data available to PNNL demonstrates a significantly larger value than that assumed for RODEX4.

Table 1.1. Sensitivity analysis for thermal expansion, solid swelling, and gaseous swelling for a BWR-4 and equilibrium batches[2]

Response 1:

Because of the similar nature of the sensitivity studies requested in questions 1 and 2, the results of these studies are presented in a combined three part response at the end of question 2. Specifically, items 1a, 1b, 1c, and 1d are addressed in the first part of response 2, item 1b is further addressed in the second part and item 1e is addressed in the third part. Please refer to the response to question 2.

Question 2:

The responses provided in the November, 2006 letter did not provide the sensitivity analyses requested in RAI# 25 from the first round of RAIs. The first round RAI# 25 requested sensitivity analyses on the impact of RODEX4 model biases and variations in uncertainty on those models considered to have uncertainties in the RODEX4 statistical methodology. The first round questions suggested in RAIs #4, 5, 6, 8, 12, 13, 15, 17 and 24 that there may be biases and greater uncertainties than those considered by RODEX4. This request is intended to supplement the RAI# 25 and provide specifics on the sensitivity analyses that should be

provided for the irradiation creep model and cladding oxidation impact licensing analyses for steady-state and slow transients. Please perform the following sensitivity studies and document the results in tables similar to Tables 2.1 – 2.4.

    a. Please assume that the irradiation creep model is biased 30% (1.30*nominal) higher than currently assumed and show how this impacts column gap formation and rod pressure analysis. In addition, please assume the uncertainty in the irradiation creep model is 50% (95/95) rather than the current value of 30% and show how this impacts column gap formation, the rod pressure limit and rod pressure analyses, see Table 2.1.

Table 2.1. Sensitivity analysis for irradiation creep model for a BWR-4 and equilibrium batches[2]

    b. Please perform rod pressure (pressure limit and rod pressure analyses) and cladding strain (slow transient and fast transient) analyses assuming the thermal creep is 20% higher than assumed (1.2*nominal), see Table 2.2.

Table 2.2. Sensitivity analysis for thermal creep model for a BWR-4 and equilibrium batches[2]

c. Please perform a sensitivity analysis for cladding strain assuming the uncertainty in cladding oxidation is 25% higher than assumed (1.25*nominal), see Table 2.3.

Table 2.3. Sensitivity analysis for cladding oxidation model for a BWR-4 and equilibrium batches[2]

Response 2:

Summary

The response to questions 1 and 2 is divided into three parts.

Part 1 consists of individual fuel rod studies performed by varying a single parameter. It addresses questions 1a, 1b, 1c, 1d, 2a, 2b, and 2c. [

]

Part 2 consists of a verification of the ATRIUM 10 steady strain calculated-minus-measured results on a 95/95 basis. It addresses questions 1b, 2a, and 2c. [

]

Part 1 – Individual Rod Sensitivity Studies (1a, 1b, 1c, 1d, 2a, 2b and 2c)

Questions 1 and 2 requested various studies to assess the impact of assumed biases or increased uncertainty ranges for the model parameters shown in Tables 1.1 and 2.1 through 2.3. The parameters from the various tables in these questions are:

[

•   ]

[

]

References

2.1   D. G. Martin, "The Thermal Expansion of Solid UO_2 and (U, Pu) Mixed Oxides - A
       Review and Recommendations," J. Nucl. Mat., No.152, 1988, pp. 94-101

2.2   J. K. Fink, "Thermal Expansion of Solid Uranium Dioxide", International Nuclear Safety
        Center, ANL web site http://www.insc.anl.gov/matprop/uo2

Table 2.4 Maximum Rod Pressure Sensitivity Results

Table 2.5 Maximum Steady Clad Strain Sensitivity Results

Table 2.6 Maximum CRWE Transient Strain Sensitivity Results

Table 2.7 Maximum Axial Gap Sensitivity Results

Figure 2.1 Thermal Expansion versus Temperature for RODEX4 and FRAPCON

Figure 2.2 Thermal Expansion Ratio, RODEX4 / FRAPCON

Part 2 - Verification of Rod Deformation Uncertainties (1b, 2a, 2c)

Additional Creepdown Data:

The cladding creepdown verification was revised per BAW-10247Q2(P) responses 12b, 13a, and 13b to include additional 10x10 data. Since that response, additional creepdown data has been acquired and included in the evaluation. Figure 2.3 shows the creepdown data of the submittal combined with the recently acquired data.

Revised CWST Zircaloy-2 Calibration:

[

]

Table 2.8 CWSR Zr-2 Clad Creep Parameters

[

]

Revised Model Uncertainties:

[

]

Table 2.9 Clad Deformation Model Uncertainties

Measurement Uncertainties:

[

]

Table 2.10 Clad Deformation Database Measurement Uncertainties

[

]

[

]

Table 2.11 Statistical Verification for Rod Creepdown Data

Figure 2.3 Measured Creepdown Data

Figure 2.4 Calculated and Measured Creepdown Data

Figure 2.5 Calculated minus Measured Creepdown

Figure 2.6 Data Evaluation Set 1

Figure 2.7 Data Evaluation Set 2

Part 3 – Evaluation of Slow Transients with Additional Uncertainties (1e)

Quantification of Transient Uncertainties:

The temperature and ramp strain results were previously calibrated as described in EMF-3014 and BAW-10247Q2(P) Responses 5 and 15. [

]

Slow Transient Methodology:

[

]

[

]

Figure 2.8 Predicted vs. Measured Centerline Temperatures – Best Estimate

Figure 2.9 Predicted Measured Fuel Centerline Temperature Deviation – Best Estimate

Figure 2.10 Predicted vs. Measured Centerline Temperatures - Conservative

**Figure 2.11 Predicted – Measured Fuel Centerline Temperature
Deviation versus Local Exposure - Conservative**

Figure 2.12 Cladding Strain Increment at Mid-Pellet from Ramp Test

Figure 2.13 Cladding Strain Increment at Pellet-End from Ramp Test

**Figure 2.14 Strain Calibration Considering Thermal Expansion and
Conductivity and Power Uncertainties**

**Table 2.12 Uncertainty Parameters for Quantification of
Thermal and Ramp Test Calibrations**

**Table 2.13 Slow Transient CRWE Results Summary
BWR-4 Transition, UO_2-Gd_2O_3 Rods , 2nd cycle**

Question 3:

Please provide the margins to the column gap formation, rod pressure, and fast and slow transient strain and fuel melt limits using the old methodology for a given design using the same fuel batch and core as performed using the new methodology. Table 6.9 of BAW-10247 provides some of these margins except for the fast and slow transients. Please compare these margins to those utilizing the new methodology and confirm that all analyses are for the same fuel batch and core. Please discuss what changes in methodology accounts for the margin difference between the old and new methodology.

Response 3:

The BWR-4 transition cycle analysis results for the RODEX2A and RODEX4 methodologies are compared for the same fuel batch and core. The BWR-4 analysis is for a 110% EPU cycle. The RODEX4 methodology results were updated for this response. The updates include RODEX4 corrections, an improvement of the RODEX4 cladding creep and pellet accommodation benchmarking and the additional uncertainties (see (BAW-10247Q4(P)) response 2). The channel bow uncertainty was not included. The comparative RODEX4 and RODEX2A/COLAPX results are summarized in Table 3.1.

[

]

[

]

Table 3.1 BWR-4 (EPU) Comparative Methodology Results

---

c   At burnup of minimum margin in RODEX2.

Table 3.2 Summary of Typical Margin Impact of Changing to RODEX4

Question 4:

The November 2006 response did not perform the rod pressure analyses that were requested in the first round RAI # 29a and 29b to demonstrate the impact of a slow power transient (due to an AOO such as a CWRE). The GDC 10 requires that fuel failure not be allowed for normal operation and AOOs. Therefore, slow power transients due to AOOs have been required for rod pressure analyses for all PWR and BWR fuel vendors in the past that perform best estimate analyses of rod pressure with a statistically derived bound. In addition, PNNL has examined the RODEX4 FGR predictions of experimental rods that have been power ramped. These comparisons to FGR data shows that RODEX4 underpredicts FGR from the power ramped rods. A comparison is also made to the RODEX4 transient release predictions presented in the response to RAI# 7e from the first round of RAIs (Figures 4.1 and 4.2) with those predicted with the FRAPCON-3.3 gas release model for the same Atrium10 design. These comparisons demonstrate that RODEX4 predicts significantly lower FGR than FRAPCON-3.3 by a factor of 1.5 or greater depending on the rod power and burnup level (see Figures 4.1 and 4.2 for burnups of 30 and 60 GWd/MTU, respectively). The RODEX4 FGR predictions provided in

response to the first round RAI#7 also demonstrates that RODEX4 has a significant dependence on grain size such that has not been demonstrated by comparisons to FGR data with differing grain size. In addition, the grain size used for the Atrium 10 design is significantly larger than 90% of the FGR data. Please provide a plot of predicted minus measured fission gas release as a function of grain size for the rods in the fission gas release assessment database. Also please provide a plot of predicted divided by measured fission gas release as a function of grain size for these same rods.

Therefore, the RODEX4 predictions of FGR need to be increased (can be accomplished by various means such as increasing the diffusion coefficient and/or fixing the grain size to a small value). Please perform a rod pressure analysis assuming a slow power AOO transient has occurred that results in the highest FGR. Please provide the input and output details of this calculation such that an audit calculation can be performed with FRAPCON similar to the information provided in Round 1 RAI #32. Please show either; a) how existing conservatisms in the rod pressure analysis bound the possible rod pressure increase due to AOOs, or b) propose how AOO transients will be included in the rod pressure analysis.

Figure 4.1 Reproduction of Figure 7e-5 from first round of responses with FRAPCON-3.3 predictions added at equivalent power and burnup.

Figure 4.2 Reproduction of Figure 7e-7 from first round of responses with FRAPCON-3.3 predictions added at equivalent power and burnup.

Response 4:

Introduction

The response to this question is broken up into several parts. In the first part it is shown that RODEX4 provides good predictions of fission gas release (FGR) in the range of interest and beyond. In the second part the FGR model with respect to grain size is addressed. In the third section, the evaluation of the rod pressure using the AOO slow transients is discussed.

Part 1 The RODEX4 FGR Predictions

The sub-set of the FGR database that consists of power ramps was thoroughly analyzed with respect to power and manufacturing uncertainties. An optimized sub-set was then defined, consisting of the most reliable transient data cases. The initial appearance of an under prediction of fission gas release is shown to be due to poor measurement data.

One of the main considerations in the selection process was the accuracy of both the rod average power value and the axial power profile. In some cases, the axial power profile was provided with only a few points and in other cases, there was a large uncertainty with respect to its shape and the peak power location. These factors contributed to a power uncertainty greater than the typical 5% standard deviation.

[

]

[

]

The results of the RODEX4 benchmarking on this optimized transient FGR data set for FGR
greater than 5% are shown in Figure 4.3 on a logarithmic scale and in Figure 4.4 on a linear
scale. The statistics of the two benchmarking measures, namely, the (predicted/measured)
ratio and the logarithm of (predicted/measured), are presented in Table 4.1.

[

]

[

]

In addition, Figure 4.8 in the original submittal, BAW-10247(P), shows the RODEX4 FGR calculated to measured comparisons for our commercial database. This plot shows excellent, best estimate, agreement with the measured data and provides further evidence that the RODEX4 FGR model provides good FGR predictions over a wide range of conditions.

While investigating the differences in FGR predicted by RODEX4 and FRAPCON-3 for the hypothetical audit power ramps of Q7e, it was discovered that the FRAPCON-3 runs performed by PNNL used a higher fuel enrichment. This caused a different radial power profile and finally led to higher fuel temperatures in the FRAPCON-3 runs. [

]

Re-runs of the audit power ramps were performed with a reduced grain size of [
]. In addition the oxidation rate was increased in the RODEX4 runs to make the temperatures closer to the temperatures in FRAPCON-3, as illustrated in Figure 4.13. This makes possible a direct comparison of the FGR predictions of the two codes with a similar temperature distribution. The results are presented in Figure 4.14 and show very good agreement.

Part 2 Grain size Dependence of FGR in RODEX4

The dependence of the FGR on the grain size in RODEX4 is consistent with the experimental data base. The diffusion of gas atoms takes place inside the grain to the grain boundary. A similar modeling was adopted in FRAPCON-3, but in it the grain size is kept constant.

[

]

[

]

As shown in the part 1 response, the excellent agreement between the predicted fuel rod FGR and the measured FGR, over the production range seen for the ATRIUM-9 and ATRIUM-10 fuel, serves as verification that the grain size dependence is being adequately modeled.

Part 3 Rod Pressure Analysis With AOO Slow Transients

[

]

The duration of the high power dwell time of the CRWE scenario is 4 hours. There are two well characterized power ramps in the RODEX4 database with a short hold time that makes them relevant for the validation of the fission gas release calculation during CRWE events. One is the GE-7 case from Super-Ramp 2 international program, with a 4 hour hold time and the other is the REGATE L-3 test with a hold time of 1.5 hours. Table 4.2 shows excellent agreement between RODEX4 predictions and measured values (the two measured values for the REGATE case represent the Kr-85 gamma scan and the puncturing values, respectively) for these two tests. This validates the application of RODEX4 to the CRWE analysis with respect to the transient fission gas release during large and short power ramps.

Another way of validating the FGR prediction by RODX4 during short hold time power transients, was to compare with FRAPCON-3 for a grain size of 10.7 MLI, which is closer to the fixed grain size in FRAPCON-3. The hypothetical audit power ramps of Q7e were limited to a 4 hours hold time and the results obtained with RODEX4 and FRAPCON-3 are presented in Table 4.3. It can be concluded that very good agreement exists between the two codes with respect to the transient FGR during short hold time transients.

Table 4.1 Optimized Transient FGR dataset Statistics

Table 4.2 Simulation of short hold time transient FGR

Table 4.3 RODEX4 comparison to FRAPCON-3 for short hold time transients

Figure 4.3 Transient FGR Results, Logarithmic Scale

Figure 4.4 Transient FGR Results, Linear Scale

Figure 4.5 Transient FGR Results, Linear Scale, with LHGR and
Diffusion Coefficient Biased to the 95%/95% upper bounds.

Figure 4.6 3D grain sizes for the fuels in the FGR database

Figure 4.7 Mean linear intercept grain sizes for the fuels in the FGR database

Figure 4.8 Predicted – Measured Comparison of FGR vs. Grain Size

Figure 4.9 Predicted / Measured Comparison of FGR vs. Grain Size

Figure 4.10 Nodal LHGR's during the Mark-BEB 66-2 power ramp

Figure 4.11 Nodal temperatures during the Mark-BEB 66-2 power ramp

Figure 4.12 Nodal FGR's during the Mark-BEB 66-2 power ramp
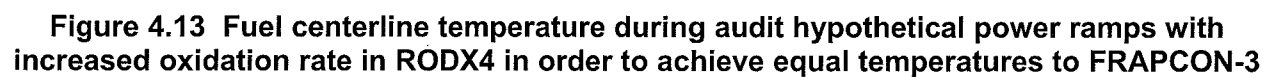
Figure 4.13 Fuel centerline temperature during audit hypothetical power ramps with increased oxidation rate in RODX4 in order to achieve equal temperatures to FRAPCON-3

Figure 4.14 RODEX4 to FRAPCON-3 comparison for audit hypothetical power ramps with a grain size of 10.7 microns, MLI and increased oxidation rate in RODX4 in order to achieve equal temperatures to FRAPCON-3

Question 5:

Section 5.2.2 of BAW-10247 provides a range of uncertainty between planned fuel management and actual operation. The uncertainty used for RODEX4 is based on the lower value for this range in Section 5.2.2. Why should this lower value be used rather than the upper-bound value? The explanation provided in how the "Operational Flexibility Uncertainty" is applied in relation to the FDL is not clear in Appendix A of BAW-10247, an example and further explanation is needed (also see RAI #15 in relation to the FDL).

Response 5:

The operational flexibility uncertainty (OFU) accounts for differences between the planned operation and the actual operation. [

]

[

]

[

]

Figure 5.1 BWR-4 Equilibrium Cycle, Maximum LHGRs

Figure 5.2 BWR-4 Equilibrium Cycle, Power Uncertainty as Fraction of FDL

Figure 5.3 BWR-4 Transition Cycle, Maximum LHGRs

Figure 5.4 BWR-4 Transition, Power Uncertainty as Fraction of FDL

Figure 5.5 BWR-6 Equilibrium Cycle, Maximum LHGRs

Figure 5.6 BWR-6 Equilibrium Cycle, Power Uncertainty as Fraction of FDL

Figure 5.7 BWR-6 Transition Cycle, Max LHGRs

Figure 5.8 BWR-6 Transition, Power Uncertainty as Fraction of FDL

Figure 5.9 BWR-6 Equilibrium Cycle, Top 10 Adjusted Power Histories, Normalized

Figure 5.10 BWR-6 Equilibrium Cycle, Top 10 Adjusted Power Histories

Question 6:

The mean input and standard deviation for the fabrication parameters appears to be based on recent historical data for the past one to two years. It is known that the mean of fabrication data can shift with time depending on several factors including machine wear, drift in calibration and other factors such that the mean can vary significantly within the specification range. This may be true even though the standard deviation does not significantly change. This can result in a significant bias in the parameter that could impact the analysis. Therefore, the statistics of the mean fabrication parameter of each batch need to be continually verified to ensure that they do not significantly vary from that assumed in the RODEX4 analyses. In addition, the standard deviation can change with time also due to machine wear or a change in machinery or other factors. This is of concern because the RODEX4 standard deviation is not based on the fabrication specification range but rather on recent experience. Therefore, the standard deviation needs to be continually verified to demonstrate that it does not significantly vary from that assumed in the RODEX4 analyses. Please define the allowable limits of mean and standard deviation variation based on sensitivity analyses or other proposed methods and propose a methodology for how these new values of mean and standard deviation will be determined and implemented if a change is necessary.

Response 6:

The BAW-10247(P) submittal contained manufacturing data from the 2001 time frame. In the response to Question 26 of the first RAI, (BAW-10247Q1(P)), additional manufacturing data were presented for the purpose of evaluating possible correlations between different manufacturing parameters. The additional data included some of the pellet and cladding manufacturing parameters for the 2005/2006 time frame.

[

]

[

]

[

]

Table 6.1 Summary of Manufacturing Parameters

Table 6.2 BWR-6 Equilibrium Core Calculations Varying Manufacturing Uncertainties

Table 6.3 Batch Variation Summary of Manufacturing Parameters

Question 7:

Based on the FRAPCON-3 audit calculations of the power ramps performed in response to Round 1 RAI #7e, it appears that RODEX4 significantly underpredicts the centerline temperature relative to FRAPCON-3 (115°C-170°C) with the differences being greater at the higher ramped powers for the cases at 30 GWd/MTU. However, the two codes predict very similar results at 60 GWd/MTU. It has been noted that the thermal conductivity in RODEX4 is about 15-7% greater than in FRAPCON-3 at 20-40 GWd/MTU. The maximum temperature case provided in response to Round 1 RAI #32 did not contain any power ramps close to or above the LHGR limit. Please provide input and output similar to the information provided in Round 1 RAI #32 for fuel melt and strain increment (output for strain increment should include elastic + permanent and the permanent only) audit calculations of feedwater controller failure, Table 6.8 of BAW-10247(P). This will allow PNNL to determine if RODEX4 provides adequate predictions of temperature at high LHGR and strain increment levels, and determine if RODEX4 will provide conservative predictions of fuel melting and strain margins. Please provide these calculations at 20, 40 and 60 GWd/MTU for a FDL Set back of 70% or less.

Response 7:

The temperature calculations reported in the response to Q4, showed that FRAPCON-3 calculates higher temperatures than RODEX4 by up to 100 °C at 30 MWd/kgU. However, at 60 MWd/kgU, RODEX4 calculates higher temperatures than FRAPCON-3 by up to 60 °C.

The RODEX4 benchmarking of the Halden temperature database is illustrated in Figure 5.36 of BAW-10247(P) as (prediction/measurement) vs. burnup. There is no bias for the whole burnup range which includes the two burnup values selected for the case studies requested in Round 1 RAI Q7, which are referred to in this question. Comparisons to measured data are more appropriate than code-to-code comparisons. Thus, it is concluded that RODEX4 properly evaluates the temperature distribution over the whole burnup range.

The cases corresponding to an FDL set back of 70% or less, from Table 6.8 of BAW-10247(P) are: 1 to 4 and 7. These cases are presented below as the results of the worst-case combination of the parameters which are subject to uncertainty for AOO fast transients.

As described in Section 3.4.5, RODEX4 is run using a steady-state power history with one axial node running along the FDL line, or a fraction of it according to the FDL set back. The input data for this run are presented in the "input_fdl_uo2" and "input_fdl_gad" files, for the UO_2 and UO_2-Gd_2O_3 fuels, respectively. The power history is listed in the "ftn24" files for each of the cases requested.

A special RODEX4 module is activated after each 1 MWd/kgU burnup increment along the FDL power history (or scaled down power history based on the FDL setback). This special module performs a side (i.e. not feeding back into the main RODEX4 calculation) transient thermal conduction calculation coupled with a thermal-elastic analysis for a given power transient. The transient relative power history is given in the files called "xtrans" for each of the requested cases. The structure of the "xtrans" file is:

- 1st line: the total number of power entries
- 2nd line: final time[s]
- 3rd line: time step[s] – RODEX4 parameter
- Next lines: time[s] and relative power

The parameters which are treated with uncertainties are those listed on p. 6-19 of BAW-10247(P). The uncertainties used for these parameters are listed in the files "xtrinp1s" and "xtrinp1m" for the maximum strain and maximum central temperature, respectively. The only difference is that the last two power parameters have been combined into a single power parameter (using the square root of sum of squares rule). The first four and the last parameters are relative values which need to be multiplied by the standard deviation (see Table 5.5 of BAW-10247(P)).

The results are presented in the files "aoodet1" and "aoodet2" for the maximum strain and the maximum temperature, respectively, for all the requested cases. The second column lists the burnup, the third column lists the elastic + plastic hoop strain (%) and the fourth column is the centerline temperature [°C]. The aoomax1 and aoomax2 contain on the second and third columns the overall maximum strain and temperature values.

Question 8:

The coefficients for the UO$_2$ fission gas release model are given in EMF-3014(P) but no mention is made of coefficients for UO$_2$-Gd$_2$O$_3$. Are the coefficients for the FGR model in RODEX4 the same for these two fuel types?

Response 8:

Yes, the coefficients are assumed to be the same.

Question 9:

Section 7.3 of EMF-3014 provides a discussion of the ROPE-II tests with 3 widely different values of overpressure provided for Rod K1 with values of > 10 MPa (Table 7.6), 13.8 MPa (Section 7.3.1) and RODEX4 calculated value of 19 MPa (Section 7.3.2) suggesting significant uncertainty in the exact value of overpressure for this rod. This rod is of particular interest because significant cladding creepout was measured in this rod. Please provide a discussion about the variability in the overpressure for this rod.

Response 9:

After base irradiation in the Obrigheim reactor, Rod K1 was refabricated with an extended gas plenum of 11.4 cm^3 for an active length of 310 mm. In cold conditions the plenum volume is equal to 94% of the free volume. The plenum is completely separated from the pellet stack so that its temperature could be more easily controlled during the test (336 °C). Since fission gas release was negligible during the test, the rod inner pressure was almost constant.

In the refabrication process, Rod K1 was pre-pressurized at 13.4 MPa (best estimate value calculated from the rod puncturing data). Studsvik Nuclear made an estimate of the internal pressure during the test using the perfect gas law and found 28 MPa (Reference 9.1). This corresponds to a rod overpressure of 13.8 MPa. This value is significantly higher than the value of > 10 MPa shown in the initial test specifications.

In the present version of RODEX4 it is not possible to change the plenum volume during irradiation. The RODEX4 calculation was initially performed with the initial small plenum as it existed before rod refabrication. The code predicted a rod overpressure of 19 MPa during the test. The results of that calculation are presented in EMF-3014 (Figure 7.18). The overestimate of the cladding deformation is due to the overprediction of the calculated rod inner pressure.

The ROPE-II calculations have been revisited and the error in the plenum volume identified. A second calculation was performed with the extended plenum. RODEX4 now predicts a rod overpressure of 14.7 MPa, which is in fairly good agreement with the Studsvik estimate. Since the RODEX4 calculation takes into account the gas present in the fuel rod, it is much more accurate than the Studsvik estimate. The calculated rod overpressure varied during irradiation in the range between 14.65 and 14.84 MPa (14.7 ± 0.2 MPa).

The cladding diameter results of the second calculation are shown in Figure 9.1. The figure shows that no adjustment of the cladding creep model is necessary to get a good prediction of cladding lift-off. Note that the reference point is different in Figure 7-18 of EMF-3014 and in

Figure 9.1. The irradiation was subdivided into a 70-hour first noise cycle, six 440-hour long irradiation cycles and a 20 hour final noise cycle. The cladding deformation jump during the first noise cycle has never been explained. Changing the reference point shows the cladding deformation during the long term irradiation cycles only.

Figure 9.1 ROPE-II Rod K1
Cladding Lift-off under the Effect of a Constant Rod Overpressure of 14.7 MPa

Rod K2 was also calculated with RODEX4. The RODEX4 predictions are shown in Figure 9.2 together with the measurement data. The rod overpressure during the test is 7.6 MPa.

**Figure 9.2 ROPE-II Rod K2
Cladding Lift-off under the Effect of a Constant Rod Overpressure of 7.6 MPa**

Reference 9.1: "ROPE II – Final Report of the ROPE II Project, Studsvik-ROPE II-20, September 1995.

Question 10:

The November 2006 response modified the coefficients to the RX Zr-2 axial growth model from those provided in EMF-3014. The original model was compared to axial elongation data in Figure 7.25 of EMF-3014. Please compare the model with the modified coefficients to these same data for RX Zr-2.

Response 10:

The new comparison is shown in Figure 10.1. The calculated rod elongation can only be larger than in Figure 7.25 of EMF-3014, since the latter shows the elongation with essentially no axial growth. The model parameters were optimized using the Risø data only.

Figure 10.1 Validation of Axial Elongation of Rods with RX Zircaloy-2 Cladding

Question 11:

The RODEX4 prediction of free void volume to commercial fuel rod data shows considerable scatter and overprediction in some of these data (Figure 8.2 and Table 6.3 of EMF-3014). An over-prediction is non-conservative for the rod pressure analysis. This suggests that the RODEX4 rod pressure analysis should account for an over-predictive bias in void volume or an uncertainty in this parameter. Do the uncertainty in the creep and irradiation growth model account for the uncertainty observed in the free void volume data? Also, see RAI #1 above. Please provide a figure of RODEX4 predicted-minus-measured void volume versus burnup of the commercial rod void volume data. Please discuss the overprediction and uncertainty further including possible methods for accounting for this bias and uncertainty in the rod pressure analyses.

Response 11:

The RODEX4 predicted-minus-measured void volume versus burnup is presented in Figure 11.1 for the commercial database. The results show an almost best estimate response of the code except for the D24 rods at high burnup. For the D24 rods the code overestimates the free volume. The D24 fuel rods have a non-standard design with a large lower plenum in addition to the upper plenum. [

]

[

]

Figure 11.1 Validation of the Rod Free Volume

It is concluded that RODEX4 appropriately models the free void volume for traditional fuel designs for rod pressure analyses. In addition, the uncertainties on the rod free volume are adequately covered by the dimensional and creep uncertainties as shown in Figure 11.2. Figure 11.2 shows the result of conservative calculations. The conservatism has been obtained by modifying the upper plenum length, the dish volume, the cladding inner and outer diameters, pellet low burnup densification and cladding creep within the uncertainty ranges.

**Figure 11.2 Conservative Rod Free Volume Predictions with Dimensional
and Creep Uncertainties**

Figure 11.2 shows that the results are conservative for all the rods of the database. Uncertainty analysis were not performed for several European reactors / rods for which manufacturing uncertainties were not available.

Question 12:

This is a follow up to RAI #12f from the first round RAIs. Please provide creep predictions in the hoop direction for a typical 10x10 cladding for CWSR Zr-2 and RX Zr-2 at an internal pressure of 100 psi and external pressure of 1050 psi constant out to 1200 days with a typical BWR cladding (assume no PCMI) fast flux and temperature. Also perform the same predictions with an internal pressure of 2200 psi and external pressure of 1050 psi. Identify primary creep, steady-state irradiation creep and if present thermal creep. Also, please provide the calculated generalized stress and strain and the stress components for each direction.

Response 12:

RODEX4 calculations were performed for a typical ATRIUM-10 cladding subjected to the internal and external pressures specified in the question. The internal pressure of 2200 psi was increased slightly (by ~4%) to 2287 psi in order to get identical hoop stress magnitude under compressive and tensile loads, which appears to be the intent of the question. The same calculation was performed for Zr-2 CWSR and RX cladding. The RODEX4 code was modified for this special purpose by substituting the internal gas pressure calculation with an input value. A user input pellet-to-cladding gap was specified sufficiently large to remain open and avoid

PCMI throughout the calculation. Figure 12.1 shows the absolute value of the permanent diameter change under both compression and tension for the CWSR cladding and demonstrates that the tensile load results in larger strain than associated with compression with the same hoop stress magnitude. Figure 12.2 demonstrates the same for RX cladding.

Figure 12.3 provides the creep components in the case of CWSR cladding under tensile hoop stress. These are the irradiation- and thermal-induced creep components. Primary creep is evident in the early thermal creep response. [

]

Table 12.1: Stress components for the creep exercise with high and low internal pressure with CWSR and RX cladding.

Figure 12.1 Diameter change due to creep for a typical ATRIUM-10 CWSR cladding with internal pressure of 2287 psi (tension) and 100 psi (compression).

Figure 12.2 Diameter change due to creep for a typical ATRIUM-10 RX cladding with internal pressure of 2287 psi (tension) and 100 psi (compression).

Figure 12.3 Diameter change due to creep for a typical ATRIUM-10 CWSR
cladding with internal pressure of 2287 psi (tension).
Irradiation- and thermal-induced creep components are shown.

Figure 12-4:   Diameter change due to creep for a typical ATRIUM-10 CWSR
cladding with internal pressure of 100 psi (compression).
Irradiation- and thermal-induced creep components are shown.

Figure 12.5 Diameter change due to creep for a typical ATRIUM-10 RX
cladding with internal pressure of 2287 psi (tension).
Irradiation- and thermal-induced creep components are shown.

Figure 12.6 Diameter change due to creep for a typical ATRIUM-10 RX
cladding with internal pressure of 100 psi (compression).
Irradiation- and thermal-induced creep components are shown

Question 13:

Does RODEX4 have a failure limit or threshold for PCI or PCMI and if so describe the model
and how is it implemented?

Response 13:

No, RODEX4 does not have a PCI or PCMI failure model.

Question 14:

[

]

Response 14:

[
                                                              ] This is explicitly stated with respect to the
SAFDL related to overheating of the cladding in Section 4.4 Thermal and Hydraulic Design of
the Standard Review Plan (1987). This section states:

"The CPB acceptance criteria are based on meeting the relevant requirements of General
Design Criterion 10 (Ref. 1.), as it relates to the reactor core being designed, with appropriate
margin to assure that specified acceptable fuel design limits are not exceeded during normal
operation or anticipated operational occurrences (AOO).

Specific criteria necessary to meet the requirements of GDC 10 are as follows:

1. SRP Section 4.2 specifies the acceptance criteria for evaluation of fuel design limits. One of the criteria provides assurance that there be at least a 95% probability at a 95% confidence level that the hot fuel rod in the core does not experience a departure form nucleate boiling (DNB) or transition condition during normal operation or anticipated operational occurrence.

Uncertainties in the values of process parameters, core design parameters, and calculation methods used in the assessment of thermal margin should be treated with at least a 95% probability at a 95% confidence level.

Two examples of acceptable approaches to meet this criterion are:

a) For departure from nucleate boiling ratio (DNBR), critical heat flux ratio (CHFR) or critical power ratio (CPR) correlations there should be a 95% probability at the 95% confidence level, that the hot rod in the core does not experience a departure from nucleate boiling transition condition during normal operation or anticipated operational occurrences; or

b) For DNBR, CHFR or CPR correlations, the limiting (minimum) value of DNBR, CHFR, of CPR is to be established such that at least 99.9% of the fuel rods would not be expected to experience departure form nucleate boiling or boiling transition during normal operation or anticipated operational occurrences."

[

]

[

]

Figure 14.1 BWR-6 Equilibrium Cycle Gas pressure Distribution

[

]

Figure 14.2 BWR-6 110% Power Uprate Gas Pressure Distribution

Question 15:

[

]

Response 15:

The crud layer thickness and composition can present large variations between different plants. They are strongly dependent on water chemistry. The prediction of the level of crud in a plant is outside the scope and capabilities of a fuel rod performance code.

Since water chemistry is not modeled in RODEX4 and the water chemistry of a specific reactor can be modified without notice by the utility even after the reload analysis is completed, crud deposition is not applied in the realistic fuel rod methodology.

In RODEX4 the crud layer can be modeled as an additional resistance between the coolant film and the corrosion layer. A crud heat transfer can be input and changed with burnup. Special crud studies can therefore be performed with RODEX4 on a plant specific basis if a customer believes that their plant has sufficient crud to require accounting for in the fuel rod analysis.

Question 16:

This is a follow-up to the AREVA response to RAI# 17 d. The hydrogen pickup fraction used in RODEX4 is more than a factor of 2 lower than the value used by FRAPCON-3.3 and as recently presented in the open literature. The response has provided a small amount of hydrogen pickup fraction with a large scatter and a value as high as 0.29. A recent search of the open literature by PNNL has demonstrated a very large range of pickup fractions in BWR Zr-2 cladding that appear to be a function of burnup with the highest pickup fractions above those used by FRAPCON-3 at burnups of 75 GWd/MTU (see References 1 and 2). It is apparent that the BWR operating parameters that impact the pickup of hydrogen in BWR cladding is poorly understood. A conservative pickup fraction is recommended for licensing analyses until hydrogen pickup in BWR Zr-2 cladding is better understood. Please provide hydrogen pickup data along with a proposed pickup fraction that bounds these data.

Response 16:

Recent publications such as Reference 16.1 indicate that

- At low burnup the hydrogen pickup fraction in BWR Zircaloy-2 is relatively high (up to 30%), but the hydrogen content in the cladding remains low (<50 ppm);

- At intermediate burnup the pickup fraction drops to values below 0.12, while the hydrogen content increases moderately;

- At high burnup (> 50 MWd/kgU) the pickup fraction may increase rapidly, while the hydrogen content may reach values in the hundreds ppm.

The data presented in the AREVA NP response to RAI# 17d are consistent with the above observation.

In the present version of RODEX4, the hydrogen content is calculated and printed for information only. The H content has no effect on the thermal-mechanical calculation. The value of the pickup fraction in RODEX4 is therefore not significant. If a limit is placed on hydrogen content in the future then a revision to the RODEX4 methodology may be necessary.

Reference 16.1: H. Hayashi et al., "Outside-in Failure of High burnup Fuel Cladding and Evaluation Tests of the Mechanism," 2005 Water Reactor Fuel Performance Meeting, Kyoto, Japan, October 2-6, 2005.

Question 17:

PNNL does not understand how either the cladding creepdown or the strain increment are calculated because the RODEX4 calculated values do not appear to make physical sense. How is the strain increment calculated in Tables 6.2, 6.3, 6.4 and 6.6 of BAW-10247, please provide elastic and plastic strains (or total and plastic)? Figure 17.1 shows the results of the BWR-4 CW-SRA UO$_2$ Max Strain audit calculation. The attached figures are proprietary and will be removed in the non-proprietary version of RAIs.

[   ]

[

]

Figure 17.1 Max power node permanent hoop strain for the BWR-4 CW-SRA UO₂ Max Strain audit calculation

Figure 17.2 Contact pressure for the BWR-4 CW-SRA UO₂ Max Strain audit calculation

Response 17:

The BWR-4 CW-SRA UO_2 Max Strain Calculation involves moderate and strong PCI, as well as trapped stack. In Figures 17.3 through 17.8 the following variables are shown to help the analysis:

Figure 17.3: Local (node 6) LHGR in kW/m versus time

Figure 17.4: Local (node 6) radial gap at mid pellet and pellet end in μm versus time

Figure 17.5: Axial power distribution change at 620 days in kW/m

Figure 17.6: Local (node 6) hoop and axial stresses at the cladding inner surface in MPa versus time

Figure 17.7: Permanent hoop strain at node 6 in % versus time

Figure 17.8: Permanent hoop strain at node 6 in % versus fast fluence

Figure 17.3 Local LHGR at Axial Node 6

Figure 17.4   Pellet-Cladding Radial Gap at Node 6

Figure 17.5 Power Axial Distribution Change at 620 days

Figure 17.6 Stresses in the Cladding at Node 6

Figure 17.7 Permanent Hoop Strain at Node 6 versus Time

[

Figure 17.8 Permanent Hoop Strain at Node 6 versus Fast Fluence

[

]

[

]

Question 18:

Round 1 RAI #11c stated that RODEX4 has not been compared to creep collapse measurements. In order to approve this model, please provide an example calculation of axial gap formation using both COLAPX and RODEX4.

Response 18:

Background:

RODEX4 was calibrated against creep ovality measurements. This is appropriate as the initial conditions and the performance of the rods measured for creep ovality were well characterized. The range of creep deformation is also directly applicable to the evaluation criteria as it covers the deformation cladding range to the occurrence of pellet–clad radial gap closure. This is the time at which the potential for fuel rod axial gap formation is determined.

The COLAPX code was theoretically developed. It was verified to be conservative for creep collapse relative to the calculation of actual creep collapse in uncharacterized fuel rods with approximate power histories. The criteria for the COLAPX methodology was revised in its most recent approval so that the minimum burnup of radial gap closure was set at a level that would preclude subsequent axial gap formation. This was determined to be 6000 MWd/MTU.

The pellet-clad radial gap closure behavior is better predicted with RODEX4 due to its more accurate calibration than with COLAPX.

Methodologies:

In both the RODEX4 and COLAPX methodologies the potential for axial column gap formation is determined.

In the COLAPX methodology, which consists of both RODEX2 calculations for creepdown and COLAPX calculations for creep ovality, the radial pellet-clad gap status at 6000 MWd/MTU is determined. At this burnup the cold gap must remain open to allow axial densification of the fuel column. This burnup was generically established so that significant axial gaps would not subsequently occur if PCI occurred beyond this burnup. The radial gap closure was for the cold gap without consideration of pellet densification, determined for the design power history. RODEX2/COLAPX calculates the first radial pellet-clad gap closure high in the column due to the symmetric "design" axial power profile.

[

]

Question 19:

Please provide a description of how the RODEX4 methodology will be applied to a plant that undergoes an extended power uprate (EPU). Please provide example audit calculation of rod internal pressure and cladding strain. In addition, please provide a demonstration of how the power histories will be selected for this plant analysis. Perform this example for the maximum expected power uprate.

Response 19:

An extended power uprate means an increase in the core average power. Typically the maximum local power is not increased in a plant uprate due to the local LHGR or MCPR limitations. In this situation the FDL limit remains the same, but more of the assemblies operate at higher average powers. To achieve these core powers more new assemblies are loaded, sometimes a half core, and more assemblies are discharged after only two cycles and at lower burnups.

There is no change in the realistic methodology for this situation. The development and benchmarking of the RODEX4 methodology covers operation with and without EPU. All the power histories are sampled, and the evaluations are performed for the 2995 rod sampling. The rods analyzed will typically run at higher powers to lower burnups. The extreme result will still be required to meet all the same design criteria.

The power uncertainties are established in the same manner as in a non-uprate analysis (see Response 5). The core margin at each exchange interval is used to develop a uniform uncertainty distribution for each rod over each exchange interval.

Tables 6.1 and 6.5 of BAW-10247(P) describe the core parameters for the sample problems. The BWR-4 case (Table 6.5) includes a 20% reactor power uprate. The transition cycle case is for one cycle at 3458 MWt and the two following cycles at 3902 MWt. The equilibrium case for the BWR-4 is for all cycles at EPU conditions of 3902 MWt.

As can be seen from Table 6.5 the batch size increases for the EPU conditions. In response 30c of BAW-10247Q1(P) the distribution of rod powers in the core for the BWR-4 24 month (EPU) transition cycle is shown. The results of the response to question 30c are repeated in tabular form (Table 19.1), for improved clarity. It can be seen that the higher fraction of assemblies loaded, as compared to the standard BWR-6 (Table 19.2), means a higher average distribution of rod powers and earlier fuel discharges.

Note that these power distributions are prior to the application of the reactor core, the power distribution measurement (radial and axial) and operational flexibility (radial and axial) power uncertainties. The maximum planned power in the BWR-4 case was 12.0 kw/ft.

**Table 19.1 Frequency Distribution BWR-4 (EPU) Transition Cycle Case,
Maximum Nodal Power versus Rod Burnup**

**Table 19.1 Frequency Distribution BWR-4 (EPU) Transition Cycle Case,
Maximum Nodal Power versus Rod Burnup (continued)**

**Table 19.2 Frequency Distribution BWR-6 Transition Cycle Case,
Maximum Nodal Power versus Rod Burnup**

**Table 19.2 Frequency Distribution BWR-6 Transition Cycle Case,
Maximum Nodal Power versus Rod Burnup (continued)**

References

19.1   Itagaki, N., K. Kakuishi, F. Yasuhiro, and T. Furuya (NFI) and O. Kubota (TEPCO), "Development of New Corrosion Resistance Zr Alloy HIFI," ENS TopFuel Meeting, March 16-19, 2003, Wurzburg, Germany.

19.2   K. Ohira, J. Kamimura, N. Otsuka, and S. Yamaguchi, "Recent Experience and Development of BWR Fuel at NFI," Proceedings of Water Reactor Fuel Performance Meeting in Kyoto, Japan, October 2-6, 2005.